ARTICLE

Cutting Experiment of *Fraxinus mandshurica* Using Waterjet-Assisted CO_2 Laser

Yueqiang Yu[1,3], Minzheng Jiang[1,*], Sheng Gao[1,*], Ting Jiang[1], Bakary S. Doumbia[2], Bo Yan[1], Tingang Ma[1], Kexin Ren[1] and Yinsong Liu[1]

[1]College of Mechanical Science and Engineering, Northeast Petroleum University, Daqing, 163318, China

[2]Forestry and Woodworking Machinery Engineering Technology Center, Northeast Forestry University, Harbin, 150040, China

[3]Research and Development Center of 3D Printing Material and Technology, Northeast Forestry University, Harbin, 150040, China

*Corresponding Authors: Minzheng Jiang. Email: jmz_1963@163.com; Sheng Gao. Email: gaosheng_7012@163.com

ABSTRACT

High-quality wood products and valuable wood crafts receive everyone's favor with the rapid development of the economy. In order to improve the cutting surface quality of wood forming parts, the cutting experiment of renewable *Fraxinus mandshurica* was conducted by waterjet-assisted CO_2 laser (WACL) technology. A quadratic mathematical model for describing the relationship between surface roughness changes and cutting parameters was established. The effects of cutting speed, flow pressure and laser power on the kerf surface roughness of *Fraxinus mandshurica* when cutting transversally were discussed by response surface method. The experimental results showed that kerf surface roughness decreased under a lower laser power, higher cutting speed and higher flow pressure. When the cutting speed was 30 mm/s, flow pressure was 1.58 MPa and laser power was 45 W, the actual surface roughness of the optimized *Fraxinus mandshurica* was 2.41 μm, and it was in accord with the theoretically predicted surface roughness value of 2.54 μm, so the model fitted the actual situation well. Through the analysis of 3D profile morphology and micromorphology, it was concluded that the optimized kerf surface of *Fraxinus mandshurica* was smoother, the cell wall was not destroyed and the tracheid was clear. It provides the theoretical basis for wood micromachining.

KEYWORDS

Green processing; waterjet-assisted CO_2 laser machining; transverse cutting; response surface method; surface roughness

1 Introduction

Laser processing is of advantages such as rapid processing speed, less waste, high precision, and desired surface quality [1–4]. Therefore, it is widely used for cutting, engraving, drilling, and surface treatment [5–8]. Environmentally friendly wood has a wide application in fields of furniture, crafts, construction and so on [9–12]. Especially, high-quality wood products and valuable wood crafts receive everyone's favor [13]. Due to the extreme shortage of wood, it is necessary to improve the high precision and utilization rate of wood resources [14,15]. Thus, laser processing is used to machine wood [16–18].

Fukuta et al. studied drilling holes in wood with lasers of different wavelengths and clarified the process mechanism. The heat-affected zone surrounding the holes was not recognized when the hole diameter on the

surface was about 20 μm [19]. Yusoff et al. studied the influence of different parameters on the processing index by cutting different kinds of wood using the CO_2 laser and obtained the optimal process parameters [20]. Eltawahni et al. demonstrated the effect of laser power, focus location and speed on cutting width surface roughness of MDF by CO_2 laser [21]. Barcikowski et al. discussed the relationship between the heat-affected zone and process parameters of wood and wood composites using the laser process [22]. However, due to the low ignition point of wood and the high temperature of laser focusing, a part of the laser energy density is always lower than the temperature of wood gasification, resulting in the burning marks and carbon residues on the surface of wood by laser machining, which seriously affects the surface quality of valuable wood products [23]. Therefore, a new laser machining method is in urgent need to perfect the surface quality of wood machining.

Yang et al. raised the waterjet-assisted YAG laser machining of wood, the results showed that with the waterjet-assisted system, the minimum value of the cutting width was 0.18 mm when the cutting speed was 50 mm/s and the laser power was 6 W, and good surface quality was obtained [24]. Moreover, the mechanism of waterjet-assisted YAG laser machining of wood was clarified to obtain the needed machining surface [25]. However, through an in-depth study, Jiang et al. found that wood had a better absorptivity of CO_2 laser waves, as well as this type of laser had a lower price. In order to study the influence of process parameters on the surface quality, Korean pine was used as the material, and the waterjet-assisted CO_2 laser (WACL) technology was used to cut the Korean pine by five factors and four levels of the orthogonal test design method. The effects of laser power, cutting speed, water pressure, defocusing amount and jet angle on the kerf width of Korean pine molded parts were discussed by range analysis method, and the optimal process parameters were determined [26]. Surface roughness is also an important index to measure machining surface quality [27].

Many recent works revealed the influence of parameters on surface quality during laser processing [28,29]. However, these variation laws of laser processing may not be suitable for WACL machining *Fraxinus mandshurica*. Especially, when processing special-textured wooden crafts, it is necessary to study cutting transversally. The purpose of this research is to investigate the surface quality of *Fraxinus mandshurica* by WACL when cutting transversally. The Box-Behnken design (BBD) was used to examine the influence of interactive effects of cutting speed, flow pressure and laser power on the surface roughness Ra of machined parts. Additionally, the predicted models were established, and then optimal process parameters were obtained. Following that, the kerf surface microstructure and 3D profile morphology of *Fraxinus mandshurica* were analyzed. A flow chart of the work stages is shown in Fig. 1.

2 Experiment

2.1 Equipment and Materials

The whole test process of WACL machining *Fraxinus mandshurica* is carried out in the WACL equipment. The equipment is composed of a CO_2 laser cutting device and a waterjet-assisted device. The CO_2 laser cutting device with a CO_2 laser generator wavelength of 10.6 μm and the rated power of the laser is 80 W (Baomei Technology Ltd., Jinan, China). The waterjet-assisted device is designed and manufactured by the authors. It is mainly composed of a QL-380 pump with the highest flow pressure of 8 MPa and nozzle with a diameter of 0.5 mm and an adjustable direction angle produced by Harbin Hongyuan Mechanical and Electrical Equipment Company (China). WACL equipment is shown in Fig. 2a.

Fraxinus mandshurica is widely applied in furniture and woodware due to its tenacity, corrosion resistance and beautiful texture. *Fraxinus mandshurica* was selected for the WACL machining test and produced in Xiaoxinganling, Heilongjiang Province. The sample size of *Fraxinus mandshurica* is 100 mm × 60 mm × 2 mm (length × width × thickness), the air dry density is 0.78 g/cm^3, and the moisture content is 12.42%. *Fraxinus mandshurica* specimens and their cutting methods (transverse cutting) are in Fig. 2b.
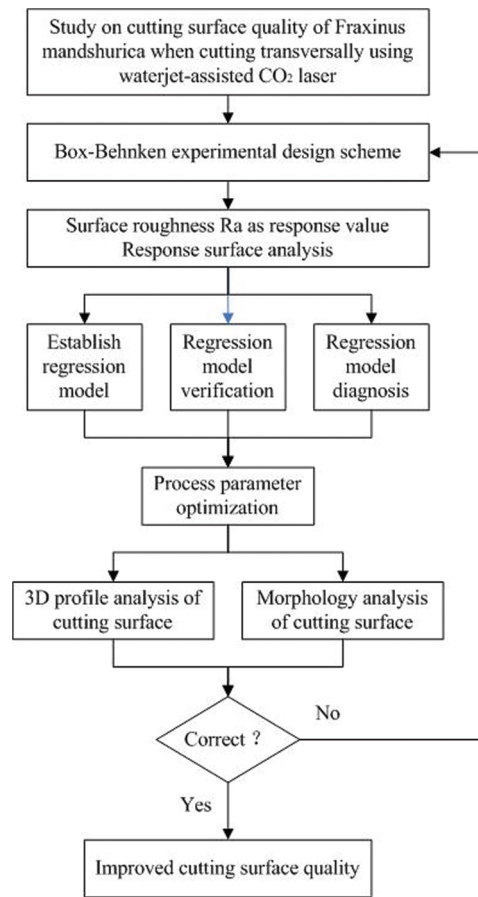
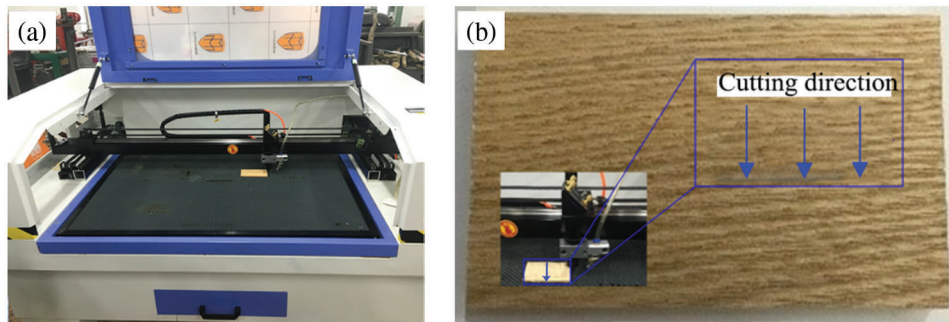**Figure 1:** A flow chart of the work stages

Figure 2: Equipment and processing ways (a) WACL equipment (b) Cutting direction of *Fraxinus mandshurica*

In the process of WACL machining *Fraxinus mandshurica*, when the temperature reaches the decomposition temperature of the wood, the wood begins to decompose and even carbonize, making the processing area of the wood to be processed produce water vapor, waste gas, carbon residue and other residues. At the same time, the waterjet can reduce the heat-affected zone and take away residuals, thus improving the surface quality of wood.

The surface roughness of the cross-section of WACL machining *Fraxinus mandshurica* was measured by Axio Scope. A1 laser microscopic system produced by Zeiss Company (Germany). Each Ra measurement was repeated three times along three different directions to achieve validity and accuracy. The average of the three replications was taken as the surface roughness value.

2.2 Experimental Design Scheme

Response surface method (RSM) is a nonlinear regression analysis method, which combines statistical principles and experimental design methods. It can model and analyze multiple input values, so as to clarify the relationship between input values and response values. The response surface method can synthesize the experimental data into linear or quadratic polynomial models to find suitable process parameters, which is convenient to solve the problem of multiple independent variables. This method can build successive variable surface models, which can assess the factors affecting the response value and their interaction, so as to determine the optimal range of factors, and then complete the optimization of parameters. Moreover, the required number of test groups is small, which can save the cost of the test, so the response surface method has been widely used.

2.3 Box-Behnken Design

The Box-Behnken design (BBD) is relatively economical, because the parameter values assortments contain combinations in moderate conditions in contrast with the full-factorial design (FFD) that includes all combinations [30]. Therefore, the Box-Behnken design scheme was selected in this paper to optimize the process parameters. Through single-factor test results, three key factors were determined by considering the influence of various factors on the kerf surface roughness of *Fraxinus mandshurica* when cutting transversely during WACL machining. Box-Behnken experimental design method (BBD) was used to analyze cutting speed (X_1), laser power (X_2) and flow pressure (X_3) as independent variables and kerf surface roughness of *Fraxinus mandshurica* as dependent variable (Y). The experimental scheme was performed using Design-Expert software (V8.0.6). The defocusing distance is −0.5 mm and the flow angle is 60°. The Box-Behnken factors and levels of the WACL machining test are in Table 1.

Table 1: Experimental design factors and levels

Level	Factors		
	Cutting speed (mm/s) X_1	Laser power (W) X_2	Flow pressure (MPa) X_3
−1	24	45	1.0
0	27	50	1.3
1	30	55	1.6

After using the BBD design scheme of the response surface method to complete the experiment, the relation equation between the response value and the independent variable was fitted by the least square method for regression analysis:

$$Y = \beta_0 + \sum_{i=1}^{3} \beta_i X_i + \sum_{i=1}^{3} \beta_{ii} X_i^2 + \sum_{i=1}^{2} \sum_{j=i+1}^{3} \beta_{ij} X_i X_j \tag{1}$$

where Y stands for response value; X_i, X_j stand for independent variables; β_0 stands for a constant term; β_i, β_{ii} are coefficients of the first and second terms; β_{ij} stands for interaction term coefficient.

3 Results and Discussion

3.1 Establishment of Regression Model

The surface roughness Ra of *Fraxinus mandshurica* when cutting transversely was used as the evaluation index, and the response surface analysis of 17 test points with three factors and three levels in Box-Behnken experimental design was used to optimize the waterjet-assisted laser processing technology with 12 test points and 5 zero points. Response surface experimental design and results was demonstrated in Table 2.

Table 2: Experimental design and results

Standard order	Factors			Response value
	Cutting speed (mm/s)	Laser power (W)	Flow pressure (MPa)	Surface roughness Ra (μm) by cutting transversally
1	30	50	1.6	3.62
2	27	50	1.3	4.18
3	27	50	1.3	4.13
4	24	45	1.3	3.23
5	27	50	1.3	4.12
6	27	45	1.0	3.84
7	27	50	1.3	4.11
8	30	55	1.3	3.91
9	24	50	1.6	5.12
10	27	55	1.6	4.92
11	24	55	1.3	5.16
12	27	55	1.0	4.54
13	27	50	1.3	4.15
14	27	45	1.6	3.00
15	24	50	1.0	5.08
16	30	45	1.3	2.90
17	30	50	1.0	4.42

The experimental data in the equation was analyzed by multiple regression, and the prediction response of surface roughness of *Fraxinus mandshurica* when cutting transversally can be calculated by second order polynomial equation:

$$Ra = -32.5906 + 0.3028X_1 + 1.576X_2 - 11.7506X_3 - 0.011X_1X_2 - 0.25X_1X_3$$
$$+ \ 0.16X_2X_3 + 7.556X_1^2 - 0.0135X_2^2 + 3.811X_3^2$$

where Y stands for response value; X_1 represents cutting speed; X_2 is laser power; X_3 represents flow pressure.

3.2 Model Verification

In order to evaluate the reliability of the mathematical model and the test results, variance analysis and explicitness test are needed for the results of the WACL test of *Fraxinus mandshurica* when cutting

transversally, as shown in Table 3. It can be seen from Table 3 that three factors have a great impact on the surface roughness of *Fraxinus mandshurica* when cutting transversally, and the interaction between the factors is obvious. The regression of the model is significant ($p < 0.0001$). The determination coefficient of the model is 0.9976, and the adjustment determination coefficient is 0.9946, indicating that this model can explain 97.05% of the change in the response value. The lack of fit $p = 0.1076 > 0.05$; it is not obvious, indicating that the unknown factors have little interference with the results. Hence, the fitting degree of the model is high, and the error of the test is small. Therefore, it is feasible to use this model to analyze and predict the surface roughness of *Fraxinus mandshurica*.

Table 3: Variance analysis of regression model for cutting *Fraxinus mandshurica*

Variation source	Sum of squares	Degrees of freedom	Mean square	F value	p value
Models	7.54	9	0.84	325.58	<0.0001
x_1	1.94	1	1.94	753.78	<0.0001
x_2	3.86	1	3.86	1501.08	<0.0001
x_3	0.25	1	0.25	97.91	<0.0001
x_1x_2	0.11	1	0.11	42.30	0.0003
x_1x_3	0.20	1	0.20	78.66	<0.0001
x_2x_3	0.23	1	0.23	89.50	<0.0001
x_1^2	0.019	1	0.019	7.56	0.0285
x_2^2	0.48	1	0.48	185.75	<0.0001
x_3^2	0.50	1	0.50	192.43	<0.0001
Residual	0.018	7	2.574×10^{-3}		
Lack of fit	0.013	3	4.500×10^{-3}	3.98	0.1076
Error	4.520×10^{-3}	4	1.130×10^{-3}		
Total	7.56	16			

3.3 Model Diagnosis

The coefficients of the multiple regression model are determined based on the analysis of the experimental data, and the multiple regression model is established at the same time. It is necessary to determine the coefficients of the multiple regression model. The adequacy of the multiple regression model is also studied according to the comparison between the predicted and experimental values. The research results are shown in Fig. 3. It can be seen from the figure that most test values are distributed above the predicted values, but only a few test values are distributed on both sides, demonstrating that the predicted values and the test values are relatively consistent.

3.4 Influence of Machining Parameters Interaction on Kerf Surface Roughness of Fraxinus mandshurica

The disturbance figure of kerf surface roughness of *Fraxinus mandshurica* during WACL machining is shown in Fig. 4a. It is obvious that the cutting speed, water pressure and laser power have a significant impact on the kerf surface roughness of the *Fraxinus mandshurica*, and the effect of the laser power and cutting speed on the kerf surface roughness of the *Fraxinus mandshurica* is higher than that of the water

pressure. The kerf surface roughness increases under higher laser power, mainly because increasing laser power produces more heat accumulating on the kerf surface.
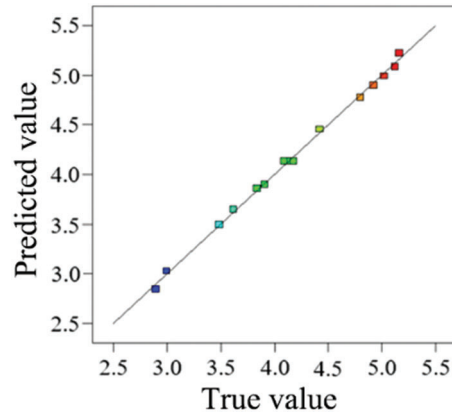

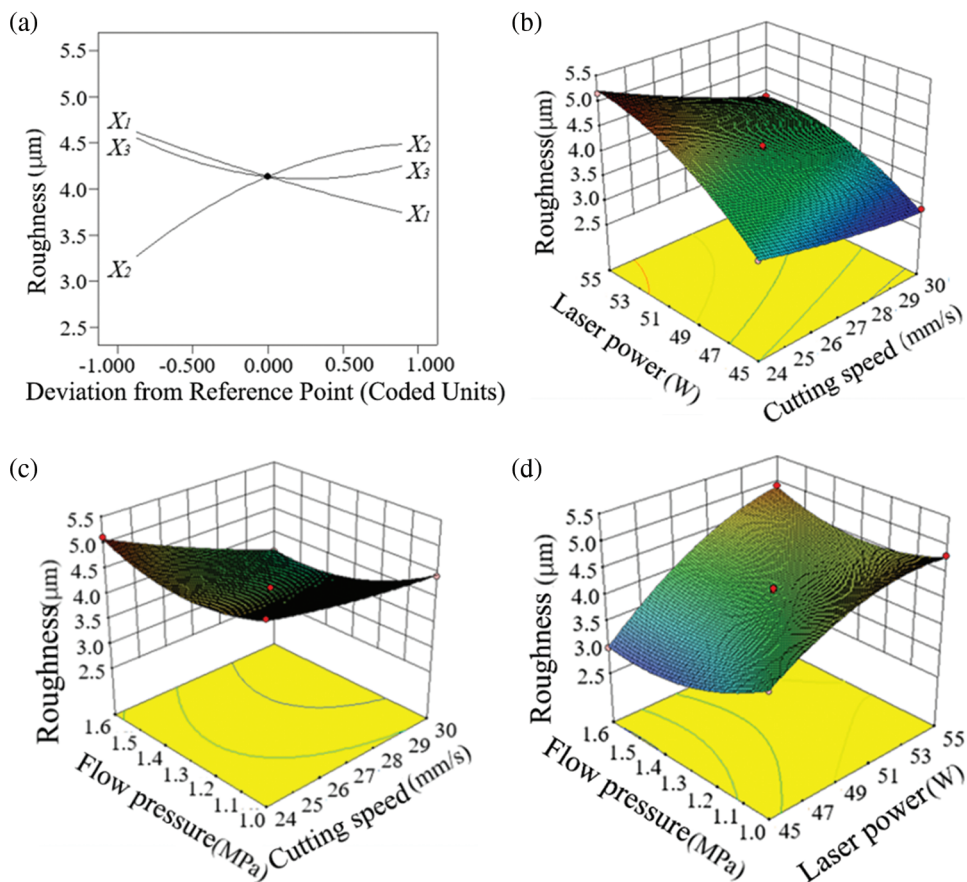**Figure 3:** Comparison chart of predicted value and true value

Figure 4: Surface roughness disturbance figure and response kerf surface figures of *Fraxinus mandshurica* (a) disturbance figure (b) laser power plus cutting speed interaction (c) flow pressure plus cutting speed interaction (d) flow pressure plus laser power interaction

Nevertheless, the roughness value decreases under higher cutting speed plus water pressure, because the laser of higher speed moves fast and less heat accumulates on the kerf surface. With the increase of water flow pressure, the turbulence and interference of water are intensified, reducing the heat of the laser on wood, so the surface roughness of *Fraxinus mandshurica* is reduced.

Machining parameters interaction also plays a key role in the surface roughness in Figs. 4b–4d. Fig. 4b shows that with a low-level cutting speed, the surface roughness is increased for larger cutting speed and the increasing rate is obvious, demonstrating the obvious effect of laser power and cutting speed interaction on surface roughness. The increasing laser power produces an amount of heat on the cutting surface of *Fraxinus mandshurica*, which leads to an increase in the surface roughness. Fig. 4c indicates the surface roughness value decreases under a larger cutting speed plus larger water pressure, and the cutting speed produces a more obvious effect on the kerf surface roughness than that of flow pressure. Fig. 4d shows the mutual effect between flow pressure plus laser power on the kerf surface roughness. Lower flow pressure and larger laser power lead to the increased surface roughness of *Fraxinus mandshurica*. In accordance with the kerf surface roughness of *Fraxinus mandshurica*, the established regression model equation was used to solve the equation, and the optimal process conditions of WACL machining *Fraxinus mandshurica* when cutting transversally were estimated: cutting speed is 30 mm/s, flow pressure is 1.58 MPa, and laser power is 45 W, and the predicted kerf surface roughness is 2.54 μm.

3.5 Result Verification

Response surface analysis was used to calculate the optimal theoretical process parameters for test to validate the reliability of BBD results. The actual surface roughness of the optimized *Fraxinus mandshurica* when cutting transversally is 2.41 μm, and it is in accord with the theoretically predicted surface roughness value of 2.54 μm, so the model fits the actual situation well.

3.5.1 Analysis of 3D Profile Morphology of Kerf Surface of Fraxinus Mandshurica

Fig. 5 shows 3D profile morphologies of the best kerf surface (No. 16 in the test) (Fig. 5a) and optimized kerf surface (Fig. 5b) of *Fraxinus mandshurica* when cutting transversally. The surface roughnesses Ra are 2.90 and 2.41 μm, respectively. Compared with the best surface roughness, the optimized kerf surface is relatively uniform and the surface roughness is small, and the surface roughness value is reduced by 16.90%. Therefore, the surface roughness decreases after optimization, producing a superior surface surface.
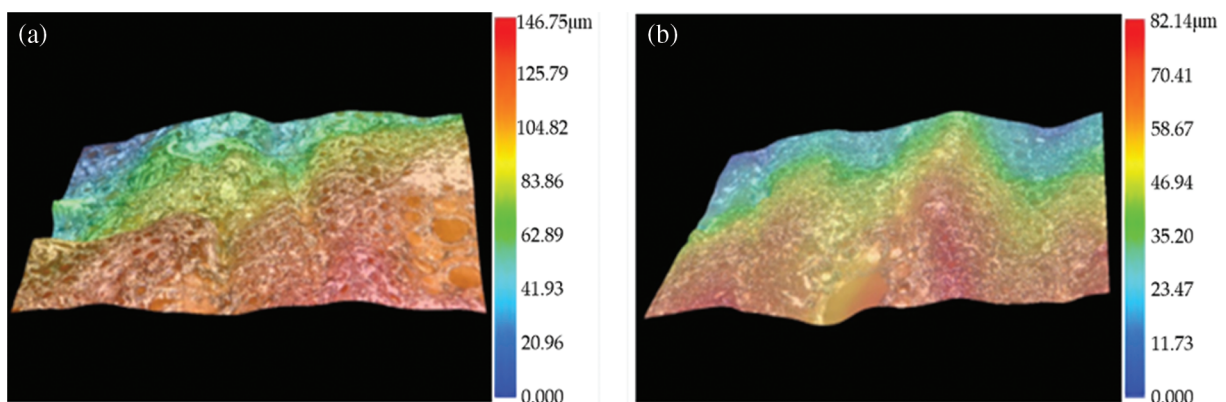

Figure 5: 3D profile morphology of kerf surface of *Fraxinus mandshurica* (a) Best kerf surface (No. 16 in the test) (b) Optimized kerf surface

3.5.2 Micromorphology Analysis of Kerf Surface of Fraxinus Mandshurica

Fig. 6 shows micromorphologies of the best kerf surface (No. 16 in the test) (Fig. 6a) and optimized kerf surface (Fig. 6b) of *Fraxinus mandshurica* when cutting transversally. Compared with Fig. 6a, in Fig. 6b the surrounding and inner wall of the vessel holes of *Fraxinus mandshurica* kerf surface are clear, with almost no residue. This is because under the optimized process parameters, the synergistic effect of each parameter makes the solid particles generated by wood vaporization taken away. At the same time, the flow of water takes away the residue, so the kerf surface quality is good.
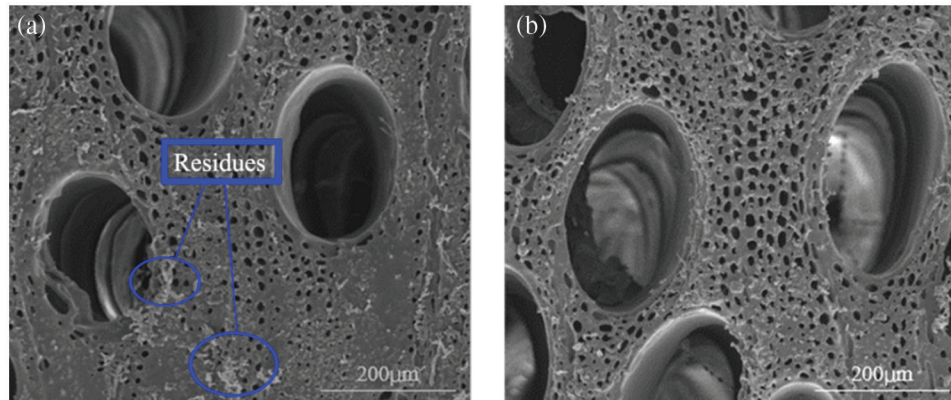

Figure 6: Microtopography of kerf surface of *Fraxinus mandshurica* (a) Best kerf surface (No. 16 in the test) (b) Optimized kerf surface

4 Conclusions

In this paper, *Fraxinus mandshurica* was cut transversally by WACL to discuss the surface quality. Surface roughness variation of machined parts followed the changes in cutting parameters. The established quadratic mathematical model for describing the relationship between surface roughness changes and cutting parameters had a good prediction effect. The model helped to select the appropriate process parameters to get the required cutting quality. The kerf surface roughness increased with the increase of laser power, but decreased with the increase of cutting speed and flow pressure. The optimal process parameters are: the cutting speed of 30 mm/s, flow pressure of 1.58 MPa, and laser power of 45 W. The predicted kerf surface roughness of *Fraxinus mandshurica* when cutting transversally was 2.54 μm, which was essentially consistent with the actual value of 2.41 μm. The analysis of 3D profile morphology and microstructure demonstrated that the surface quality of *Fraxinus mandshurica* was improved, which provides the theoretical basis to obtain the expected surface quality for wood micromachining.

Availability of Data and Materials: The data that support the findings of this study are available from the corresponding authors upon reasonable request.

Conflicts of Interest: The authors declare that they have no conflicts of interest to report regarding the present study.

References

1. Rezayat, M., Aboutorabi Sani, A., Talafi Noghani, M., Saghafi Yazdi, M., Taheri, M. et al. (2023). Effect of lateral laser-cladding process on the corrosion performance of Inconel 625. *Metals, 13,* 367.

2. Rezayat, M., Roa, J., Mateo, A. (2022). Phase transformation and residual stresses after laser surface modification of metastable austenitic stainless steel. *International Conference on Fracture and Damage Mechanics, 9,* 1–10.

3. Sivarao, S., Ali, A., Ahmad, K. K., Pujari, S. (2022). RSM modelling for laser cutting of shore wood to replace traditional manufacturing method. *Key Engineering Materials, 908,* 526–534.

4. Moradi, M., Mehrabi, O., Azdast, T., Benyounis, K. Y. (2017). Enhancement of low power CO_2 laser cutting process for injection molded polycarbonate. *Optics & Laser Technology, 96,* 208–218.

5. Marimuthu, S., Dunleavey, J., Liu, Y., Antar, M., Smith, B. (2019). Laser cutting of aluminium-alumina metal matrix composite. *Optics & Laser Technology, 117,* 251–259.

6. Shi, C., Ren, N., Wang, H., Xia, K., Wang, L. (2018). Effects of ultrasonic assistance on microhole drilling based on Nd: YAG laser trepanning. *Optics & Laser Technology, 106,* 451–460.

7. Nikolidakis, E., Antoniadis, A. (2021). FEM modeling and simulation of kerf formation in the nanosecond pulsed laser engraving process. *CIRP Journal of Manufacturing Science and Technology, 35,* 236–249.

8. Guo, C., Wang, L., Zhou, J., Cao, B., Zhu, B. (2021). Effect of grain refinement by laser surface treatment on cell adhesion behavior of AZ91D magnesium alloy. *Journal of Testing and Evaluation, 49(3),* 201–219.

9. Ji, L. F., Zhang, Q. X., Rao, F. (2022). Engineered wood/bamboo laminated composites for outdoor hydrophilic platforms: Structural design and performance. *Journal of Renewable Materials, 10(9),* 2477–2487. https://doi.org/10.32604/jrm.2022.021761

10. Maryono, Farida, N., Ngatno, Prabawani, B. (2021). Building innovation capabilities on collaboration and market orientation for improving marketing performance of wood furniture craft. *Humanities and Social Sciences Letters, 9,* 439–451.

11. Wang, K. K., Salenikovich, A., Cloutier, A., Beauregard, R. (2009). Development of a new engineered wood product for structural applications made from trembling aspen and paper birch. *Forest Products Journal, 59(7),* 31–35. https://doi.org/10.13073/0015-7473-59.10

12. Wang, Z. (2012). An investigation on water jet machining for hardwood floors. *European Journal of Wood and Wood Products, 70(1–3),* 55–59. https://doi.org/10.1007/s00107-010-0492-0

13. Dewindiani, N. W., Suhasman, Yunianti, A. D. (2019). Colourability of wood and its effect on bonding strength of laminated wood for handicraft material. *Materials Science and Engineering, 593,* 1–7. https://doi.org/10.1088/1757-899x/593/1/012019

14. Wu, J. F., Liang, J. Y., Chen, M. Y., Zheng, S. Q., Xu, J. Y. (2023). Study on the structural characteristics and physical and mechanical properties of phoebe bournei thinning wood. *Journal of Renewable Materials, 10(11),* 3025–3039. https://doi.org/10.32604/jrm.2022.019989

15. Leone, C., Lopresto, V., Iorio, I. D. (2009). Wood engraving by Q-switched diode-pumped frequency-doubled Nd: YAG green laser. *Optics and Lasers in Engineering, 47(1),* 161–168. https://doi.org/10.1016/j.optlaseng.2008.06.019

16. Kubovský, I., Kacík, F., Reinprecht, L. (2016). The impact of UV radiation on the change of colour andcomposition of the surface of lime wood treated with a CO_2 laser. *Journal of Photochemistry and Photobiology A: Chemistry, 322,* 60–66.

17. Hernández-Castañeda, J. C., Sezer, H. K., Li, L. (2010). Dual gas jet-assisted fibre laser blind cutting of dry pine wood by statistical modelling. *International Journal of Advanced Manufacturing Technology, 50(1–4),* 195–206. https://doi.org/10.1007/s00170-009-2491-z

18. Severin, J., Manuel, J. P., Anton, H., Reinhard, P. (2017). Femtosecond laser machining for characterization of local mechanical properties of biomaterials: A case study on wood. *Science and Technology of Advanced Materials, 18(1),* 574–583. https://doi.org/10.1080/14686996.2017.1360751

19. Fukuta, S., Nomura, M., Ikeda, T., Yoshizawa, M., Yamasaki, M. et al. (2016). UV laser machining of wood. *European Journal of Wood and Wood Products, 74(2),* 261–267. https://doi.org/10.1007/s00107-016-1010-9

20. Yusoff, N., Ismail, S. R., Mamat, A., Ahmad-Yazid, A. (2008). Selected Malaysian wood CO_2 laser cutting parameters and cut quality. *American Journal of Applied Sciences, 5(8),* 990–996. https://doi.org/10.3844/ajassp.2008.990.996

21. Eltawahni, H. A., Olabi, A. G., Benyounis, K. Y. (2011). Investigating the CO_2 laser cutting parameters of MDF wood composite material. *Optics & Laser Technology, 43(3),* 648–659. https://doi.org/10.1016/j.optlastec.2010.09.00

22. Barcikowski, S., Koch, G., Odermatt, J. (2006). Characterisation and modification of the heat affected zone during laser material processing of wood and wood composites. *Holz als Roh-und Werkstoff, 64(2),* 94–103. https://doi.org/10.1007/s00107-005-0028-1

23. Kačík, F., Kubovský, I. (2011). Chemical changes of beech wood due to CO_2 laser irradiation. *Journal of Photochemistry and Photobiology A: Chemistry, 222(1),* 105–110. https://doi.org/10.1016/j.jphotochem.2011.05.008

24. Yang, C. M., Jiang, T., Yu, Y. Q., Dun, G. Q., Ma, Y. et al. (2018). Study on surface quality of wood processed by water-jet assisted nanosecond laser. *BioResources, 13(2),* 3125–3134.

25. Yang, C. M., Jiang, T., Yu, Y. Q., Bai, Y., Song, M. L. et al. (2019). Water assisted nanosecond laser microcutting of Northeast China ash wood: Experimental study. *BioResources, 14(1),* 128–138.

26. Yang, C. M., Jiang, T., Yu, Y. Q., Lou, Y. X., Liu, J. Q. et al. (2020). Water-jet assisted laser cutting of Korean pine (Pinus koraiensis): Process and parameters optimization. *BioResources, 15(2),* 2540–2549. https://doi.org/10.15376/biores.15.2.2540-2549

27. Martínez-Conde, A., Krenke, T., Frybort, S., Müller, U. (2017). Review: Comparative analysis of CO_2 laser and conventional sawing for cutting of lumber and wood-based materials. *Wood Science and Technology, 51(4),* 943–966. https://doi.org/10.1007/s00226-017-0914-9

28. Kubovský, I., Kacík, F. (2014). Colour and chemical changes of the lime wood surface due to CO_2 laser thermal modification. *Applied Surface Science, 321,* 261–267. https://doi.org/10.1016/j.apsusc.2014.09.124

29. Fountas, N. A., Ninikas, K., Chaidas, D., Kechagias, J., Vaxevanidis, N. M. (2022). Neural networks for predicting kerf characteristics of CO_2 laser-machined FFF PLA/WF plates. *MATEC Web of Conferences, 368,* 01010. https://doi.org/10.1051/matecconf/202236801010

30. Kechagias, J. D., Vidakis, N. (2022). Parametric optimization of material extrusion 3D printing process: An assessment of Box-Behnken vs. full-factorial experimental approach. *The International Journal of Advanced Manufacturing Technology, 121,* 3163–3172.